Adducin forms a bridge between the erythrocyte membrane and its cytoskeleton and regulates membrane cohesion

*William A. Anong,[1] *Taina Franco,[1] *Haiyan Chu,[1] Tahlia L. Weis,[1] Emily E. Devlin,[2] David M. Bodine,[2] Xiuli An,[3] Narla Mohandas,[3] and Philip S. Low[1]

[1]Department of Chemistry, Purdue University, West Lafayette, IN; [2]Genetics and Molecular Biology Branch, National Human Genome Research Institute, National Institutes of Health, Bethesda MD; and [3]Laboratory of Physiology, New York Blood Center, NY

The erythrocyte membrane skeleton is the best understood cytoskeleton. Because its protein components have homologs in virtually all other cells, the membrane serves as a fundamental model of biologic membranes. Modern textbooks portray the membrane as a 2-dimensional spectrin-based membrane skeleton attached to a lipid bilayer through 2 linkages: band 3–ankyrin–β-spectrin and glycophorin C–protein 4.1–β-spectrin.[1-7] Although evidence supports an essential role for the first bridge in regulating membrane cohesion, rupture of the glycophorin C–protein 4.1 interaction has little effect on membrane stability.[8] We demonstrate the existence of a novel band 3–adducin–spectrin bridge that connects the spectrin/actin/protein 4.1 junctional complex to the bilayer. As rupture of this bridge leads to spontaneous membrane fragmentation, we conclude that the band 3–adducin–spectrin bridge is important to membrane stability. The required relocation of part of the band 3 population to the spectrin/actin junctional complex and its formation of a new bridge with adducin necessitates a significant revision of accepted models of the erythrocyte membrane. (Blood. 2009;114: 1904-1912)

Introduction

The model of the erythrocyte membrane presented in cell biology, hematology, and biochemistry textbooks shows 2 major protein bridges that span between the phospholipid bilayer and the spectrin/actin skeleton.[1-7] The more prominent bridge, a linkage from the integral membrane protein, band 3, to spectrin via ankyrin, is composed of multiple high-affinity protein-protein interactions.[9-11] Defects or deficiencies in either band 3 or ankyrin lead to a decrease in cohesion between the lipid bilayer and membrane skeleton, resulting in loss of membrane surface area and a pathology termed hereditary spherocytosis.[12-14] Manual rupture of this bridge by addition of competing fragments of either band 3 or ankyrin, or by addition of competing monoclonal antibodies, or mutation of the ankyrin binding site on band 3 induces spontaneous membrane vesiculation and fragmentation.[14-16] Spontaneous mutations in the ankyrin-bridging function in other cells can also lead to serious pathologies.[17-20] Taken together, these data support the importance of the ankyrin-spectrin bridge in maintaining membrane integrity.

The second bridge connecting the membrane bilayer to the spectrin-actin skeleton consists of the membrane-spanning protein, glycophorin C (GPC), tethered to spectrin via the adapter protein 4.1.[21-23] The complex of cytoskeletal proteins at this nexus (primarily actin, dematin, tropomyosin, adducin, protein 4.1, and tropomodulin) forms a junctional complex from which spectrin tetramers extend radially into a 2-dimensional lattice that provides mechanical stability to the overlying membrane. Based on the finding that GPC-deficient red cells exhibit decreased membrane mechanical stability, it has been inferred that the GPC–protein 4.1 bridge is essential to erythrocyte integrity.[24,25] However, recent observations demonstrate that the decreased membrane stability of GPC-deficient red cells is the consequence of a secondary deficiency of protein 4.1, and that reconstitution of the spectrin-actin binding domain of protein 4.1 into these defective membranes restores membrane mechanical stability without re-establishing the tether to GPC.[26,27] Furthermore, rupture of the GPC–protein 4.1 bridge by 5 independent methods has been shown to have no obvious impact on membrane mechanical properties.[8] Taken together, one can conclude that the GPC–protein 4.1–junctional complex bridge does not play a prominent role in maintaining membrane stability.

With the functional significance of the GPC–protein 4.1 bridge uncertain, we undertook to search for an alternative membrane-to-junctional complex bridge that might contribute to membrane mechanical properties in the erythrocyte model system. We demonstrate in this study that adducin, an actin-capping protein that also binds spectrin and facilitates its association with actin,[28-30] directly binds the cytoplasmic domain of band 3 (cdb3) and thereby mediates attachment of the junctional complex to the phospholipid bilayer. We also demonstrate that rupture of this bridge leads to spontaneous membrane fragmentation and vesiculation. Because band 3 serves as the membrane-associated anchor of this new bridge, these new data require that a fraction of the band 3 population be repositioned at the junctional complex, that is, a distance of several hundred angstroms from its customary position at the ankyrin-spectrin junction.

Methods

Antibodies

Anti-cdb3, anti–glycophorin A, anti–glycophorin C, anti–glyceraldehyde-3-phosphate dehydrogenase (GAPDH), and anti–protein 4.1 were generated

Submitted February 2, 2009; accepted June 18, 2009. Prepublished online as *Blood* First Edition paper, June 30, 2009; DOI 10.1182/blood-2009-02-203216.

*W.A.A., T.F., and H.C. contributed equally to this work.

The online version of this article contains a data supplement.

The publication costs of this article were defrayed in part by page charge payment. Therefore, and solely to indicate this fact, this article is hereby marked "advertisement" in accordance with 18 USC section 1734.

in our laboratory with purified proteins. Anti–α-adducin, anti-ankyrin, and anti-spectrin were purchased from Santa Cruz Biotechnology; anti-actin was from Sigma-Aldrich; anti-His and anti–glutathione S-transferase (GST) were from GE Healthcare; and anti-CD47 was from Becton Dickinson Co.

Preparation of recombinant adducin fragments

Expression plasmids for GST fusion constructs of β-adducin tail (amino acids 335-726), β-adducin head (amino acids 1-346), intact β-adducin, and α-adducin (amino acids 1-335) head were kind gifts from Vann Bennett (Duke University). Each of these domains was expressed in *Escherichia coli* and purified on a GST column (GE Healthcare). The cDNA of α-adducin tail (430-737 aa; a gift from Vann Bennett) was cloned into the expression plasmid, pT7-7, attached to a $(His)_6$ tag at its C terminus, expressed in *E coli*, and purified using nickel-nitrilotriacetic acid beads (QIAGEN).

Label transfer studies

Intact purified human erythrocyte adducin (150-500 μg/mL) was labeled with sulfo-N-hydroxysuccinimidyl-2-(6-[biotinamido]-2-(p-azido benzamido)-hexanoamido) ethyl-1,3′-dithiopropionate (sulfo-SBED) in phosphate-buffered saline (PBS) containing a protease inhibitor mixture, per manufacturer's suggestion (Pierce Biotechnology). Bovine serum albumin (BSA) was labeled with the same reagent to serve as a control. KI-stripped inside-out erythrocyte membrane vesicles (KI-IOV; 210 μg protein) were gently mixed for 1 hour in the dark at 4°C with sulfo-SBED–adducin or sulfo-SBED–BSA. Photoactivated cross-linking of the biotinylated proteins to their binding partners was then performed by illumination for 10 minutes with a 302 nm light source (18.4 W) placed 5 cm from the sample. Dithiothreitol (10 mM) was then added to 100 μL sample to reduce the reagent's disulfide bond, and the sample was dissolved in an equal volume of 2× sodium dodecyl sulfate (SDS) sample buffer. Samples were mixed by vortexing, heated for 5 minutes at 60°C, and then analyzed by SDS–polyacrylamide gel electrophoresis (SDS-PAGE). Biotinylated proteins were identified by Western blotting using streptavidin–horseradish peroxidase (1/60 000 dilution).

Surface plasmon resonance assay

Surface plasmon resonance assay was performed using a BIAcore 3000 instrument (BIAcore). GST-tagged cytoplasmic domain of band 3 was covalently coupled to a CM-5 biosensor chip using an amino-coupling kit. The instrument was programmed to perform a series of binding assays with increasing concentrations of adducin more than the same regenerated surface. His-tagged C terminus of β-adducin was injected onto the band 3 cytoplasmic domain-coupled surface. Binding reactions were done in the buffer containing 20 mM HEPES (N-2-hydroxyethylpiperazine-N′-2-ethanesulfonic acid), pH 7.4, 150 mM NaCl, 3 mM EDTA (ethylenediaminetetraacetic acid), and 0.05% (vol/vol) surfactant P20. The surface was regenerated with 0.05% SDS before each new injection. Derived sensograms (plots of changes in resonance units on the surface as a function of time) were analyzed using the software BIAeval 3.0. Affinity constants were estimated by curve fitting using a 1:1 binding model.

GST pull-down assay

To measure the binding of β-adducin to band 3 in vitro, GST-tagged cdb3 was coupled to glutathione beads at room temperature for 30 minutes. Beads were pelleted and washed with PBS/10% sucrose buffer. His-tagged C terminus of β-adducin (tail domain) was added to the GST–band 3–conjugated beads in a total volume of 100 μL. The final concentrations of both band 3 cytoplasmic domain and β-adducin fragment were 1 μM. The mixture was incubated for 1 hour at room temperature, pelleted, and washed. The pellet was analyzed by SDS-PAGE, and β-adducin fragment was detected by Western blotting using anti-His antibody. GST and GST-tagged cytoplasmic domain of glycophorin C were used as negative controls.

KI-IOV and GST–adducin binding assay

IOVs are erythrocyte membrane preparations that have been depleted of spectrin and actin by incubation in low ionic strength buffers, but still retain all transmembrane proteins and most of the more tightly associated cytoskeletal proteins; KI-IOVs are IOVs that have been stripped of remaining peripheral proteins with 1 M KI, thus retaining primarily their normal complement of membrane-spanning proteins. These 2 membrane preparations contain the proteins that must ultimately anchor the spectrin skeleton into the lipid bilayer. Increasing concentrations of ^{125}I-labeled erythrocyte adducin, purified GST–β-adducin, or its fragments were mixed with KI-IOVs at 4°C overnight in binding buffer (PBS containing 10% sucrose, protease inhibitor mixture, and 1 mg/mL BSA). After incubation, the KI-IOV suspension was layered more than 5 volumes of a 25% wt/vol sucrose cushion and centrifuged for 45 minutes at 42 000*g*. The pellets were solubilized in 0.5% Nonidet P-40 in binding buffer, and bound adducin amount was quantified by GST activity kit (GE Healthcare) or γ counting (Packard Cobra Auto γ counter) when ^{125}I-labeled adducin was used. BSA was used as a negative control.

Competition of GST–β-adducin binding to KI-IOVs by intact adducin or anti-cdb3

Increasing concentrations of purified intact adducin or cdb3 were mixed with KI-IOVs in binding buffer and incubated on a gently revolving platform at 4°C for 4 hours. A total of 250 nM GST–β-adducin tail was then added and incubated overnight at 4°C, after which the samples were processed as described in "KI-IOV and GST–adducin binding assay."

Binding of GST–β-adducin domains to His-tagged cdb3 immobilized on nickel beads

His-tagged band 3 was immobilized on nickel beads and incubated with purified GST fusion constructs of intact β-adducin or its fragments overnight at 4°C in PBS containing 10% sucrose, protease inhibitor mixture, and 1 mg/mL BSA. Beads were washed with PBS and eluted with 250 mM imidazole, 300 mM NaCl, and 50 mM NaH_2PO_4, pH 8.0. The amount of bound fusion protein was evaluated by measuring the GST activity on the beads or by performing quantitative dot blots using anti-GST polyclonal antibody.

Binding of α-adducin tail to cdb3 immobilized on Affi-Gel 15

Cdb3 was immobilized on Affi-Gel 15, according to the manufacturer's instructions (Bio-Rad). Briefly, 20 nmol cdb3-$(His)_6$ was mixed with 500 μL packed Affi-Gel 15 (Bio-Rad) in a total volume of 2 mL. After gently mixing overnight at 4°C, unreacted Affi-Gel sites were blocked by incubating for 1 hour in 1 M ethanolamine, pH 8.0. The resulting beads were washed with ice-cold double-distilled H_2O and then equilibrated in PBS, pH 7.2. Ovalbumin was similarly immobilized onto Affi-Gel 15 as a control. Different concentrations of α-adducin tail-$(His)_6$ were incubated with the cdb3- and ovalbumin-derivatized beads for 3 hours at 4°C. Beads were pelleted, washed 3 times with PBS to remove unbound α-adducin, and analyzed by SDS-PAGE, followed by immunoblotting. α-Adducin tail fragment was detected with anti–α-adducin antibody, followed by quantitative densitometry using ImageJ software. The binding curve was fitted, and the K_D was calculated using GraphPad Prism software.

Generation of band 3 knockout mice that survive to adulthood

Two different band 3 knockout mice have been generated to date; however, because of the fragility of their erythrocytes, the pups rarely survive past childbirth.[31,32] Consequently, to obtain sufficient band 3–null erythrocytes for adducin studies, a new band 3 knockout mouse that would survive to adulthood had to be created. Band 3 knockout mice were generated through homologous recombination of embryonic stem cells. A 3227-base pair 5′ arm from the mouse Slc4a1 locus (coordinates chromosome 11: 102 472 363 to 102 469 136) that extends into exon 4 was fused to a PGK-Neo gene flanked by loxP sites and a 5232 3′ arm (coordinates chromosome 11: 102 469 136 to 102 464 304) in a modified pPNT vector.[14] Transgene expression is sometimes abrogated by an intronic neomycin cassette, which can interfere with transcription or mRNA processing. The 3′ arm contains a 33-bp deletion that removes a β-hairpin loop in exon 7 (coordinates chromosome 11: 102 467 497 to 102 467 529; supplemental Figure 1,

available on the *Blood* website; see the Supplemental Materials link at the top of the online article). The 11-amino-acid β-hairpin loop in the cytoplasmic domain of band 3 is responsible for ankyrin binding in mouse erythrocytes.[14] The targeting vector was transected into TC1 embryonic stem cells, and recombinant clones were isolated using previously described methods.[14] Approximately 12 cells from 2 clones were injected into C57BL/6J (B6) blastocysts to generate chimeric mice.

Chimeras were bred to Black Swiss female mice, and germline transmission was demonstrated by the presence of agouti pups in the F_1 litters. Polymerase chain reaction analysis of DNA from tail biopsies of F_1 animals was used to identify animals heterozygous for the targeted PGK-Neo insertion. Heterozygotes (−/+) were intercrossed to generate F_2 generation pups, which were completely band 3–deficient based on Western blot analysis of both intact erythrocytes and isolated erythrocyte ghosts. Homozygous (−/−) transgenic mice were easily detected at birth by their extreme pallor, but most survived to adulthood. Polymerase chain reaction analysis of F_2 mice confirmed that these animals were homozygous for the recombinant locus. Genetic heterogeneity in the colony was maintained by alternate backcrossing with 129 and Black Swiss mice. Complete blood counts were determined using a Coulter counter, and osmotic fragility was determined using established methods.[14] Reticulocyte counts were measured manually by staining of peripheral blood smears with Crystal Violet.

Mice homozygous for the transgene were born in a Mendelian ratio (17/74 = 22.9%), and more than 80% of homozygous pups survived to weaning. Homozygous Slc4a1$^{-/-}$ mice had a phenotype similar to previous homozygous band 3–null mice[31,32] in that they exhibited massive splenomegaly, severely reduced red cell number and hematocrit, elevated reticulocyte count, increased number of nucleated red cells, and severe osmotic fragility (supplemental Table 1). In contrast, heterozygous Slc4a1$^{+/-}$ mice had normal hematologic values, with the exception of a mild elevation in the reticulocyte count and slight osmotic fragility. All of the mice used in this study were bred, housed, and manipulated using an National Human Genome Research Institute–approved animal study protocol (G-04-2).

Analysis of adducin content of intact mouse band 3–null erythrocytes

To mimic the reticulocyte content of the above band 3–null blood, anemic wild-type blood cells were used as a control. Reticulocytosis was induced by daily phlebotomy for 4 days, resulting in an average hematocrit of 26.7% after the last bleed. Blood was collected 48 hours after the last bleed, when the average reticulocyte percentage was 58%. Mouse band 3–null erythrocytes and anemic wild-type mouse erythrocytes were gently washed 3 times in PBS and plunged into 5× SDS-PAGE sample buffer. Samples were homogenized by ultrasonication for 5 seconds and then analyzed by SDS-PAGE and immunoblotting with anti–α-adducin antibody. The same nitrocellulose membrane was then stripped of bound antibodies and reprobed with anti-actin antibody as a loading control. Quantitative densitometry was performed with ImageJ software to compare the adducin content in band 3–null and anemic wild-type erythroid cells.

Morphologic evaluation of erythrocytes resealed with increasing concentrations of adducin tail domains

Increasing concentrations of α-adducin tail or β-adducin tail domains were incubated for 1 to 2 hours on ice with leaky erythrocytes (50% Hct) in a total volume of 500 μL. Erythrocytes were then resealed for 45 minutes at 37°C in PBS either containing or lacking 4 mM Mg^{2+}. Resealed cells were washed twice with PBS and resuspended in PBS containing 5% (wt/vol) BSA before staining with Wright stain and analysis by phase-contrast microscopy (Olympus BH-12). Images were taken with an Olympus DP70 camera under a 100×/1.25 NA oil objective lens. Olympus DP controller (2.2.1.227) image-acquisition software was used.

Quantitation of band 3 retention in erythrocyte membrane skeletons from cells resealed with different concentration of adducin tail domains

Increasing amounts of His-tagged α-adducin tail or GST–β-adducin tail domains were incubated for 2 to 4 hours on ice with leaky erythrocyte ghosts (3-5 mg/mL protein) in a total volume of 500 μL. When desired, 4 mM $MgCl_2$ was added and the incubation was continued for another 30 minutes. Erythrocytes were then resealed for 45 minutes at 37°C in PBS and extracted in 1% to 2% Triton X-100 (final concentration). Membrane skeletons were then collected by centrifugation at 85 500*g* through a 25% sucrose-PBS cushion. Skeletons were analyzed by SDS-PAGE, followed by immunoblotting with anti–band 3 and anti-actin antibodies. Densitometry of band 3/actin ratios was quantitated using ImageJ software.

Results

Adducin-binding proteins in KI- IOVs can be identified by label transfer and pull-down experiments

Adducin is a peripheral membrane protein that caps actin filaments and enhances the affinity of spectrin for actin.[30] Because adducin remains partially associated with erythrocyte membranes after removal of their spectrin/actin networks, it constitutes a plausible candidate for a bridge-forming protein that might tether the junctional complex to the lipid bilayer. In an effort to determine whether adducin might perform this bridging function, adducin was purified from fresh human erythrocytes,[33] labeled in the dark with a photoactivatable cross-linking probe (sulfo-SBED), and allowed to bind KI-IOVs. After photo-cross-linking to promote biotin label transfer to nearest neighbor proteins, the labeled KI-IOV proteins were identified by SDS-PAGE, followed by streptavidin-peroxidase blotting (see "Methods"). As seen in Figure 1A, 3 distinct proteins of apparent M_r at approximately 100 kDa, 55 kDa, and 35 kDa were revealed, whereas no KI-IOV proteins were detected when sulfo-SBED–adducin was replaced with sulfo-SBED–serum albumin. By mass spectrometry, the highest molecular weight band was identified as band 3, whereas the identities of the other labeled proteins were not unequivocally established. One candidate revealed by mass spectroscopy for the 35-kDa band was stomatin, a protein of M_r at approximately 31.5 kDa that has previously been reported to bind adducin.[34]

To characterize the adducin-membrane interaction more quantitatively, we conducted direct binding studies between ^{125}I-labeled adducin and KI-IOVs. As seen in Figure 1B, adducin was found to bind KI-IOVs in a saturable manner with a K_D approximately 100 nM. In similar assays, ^{125}I-labeled BSA displayed no affinity for KI-IOVs. Because unlabeled adducin was observed to competitively inhibit ^{125}I-adducin binding to KI-IOVs with an apparent K_I of approximately 75 nM (data not shown), we conclude that adducin's association with KI-IOVs is specific and of high affinity.

Identification of the adducin domain that binds KI-IOVs

Previous work by Bennett and colleagues has established that adducin consists of 2 homologous subunits (α = 103 kDa and β = 97 kDa), each with an NH_2-terminal protease-resistant head domain (~ 40 kDa) and a COOH-terminal protease-sensitive tail domain (~ 33 kDa) connected by a small neck (~ 9 kDa).[28,35] To determine whether one of the domains of β-adducin might bind KI-IOVs, purified GST fragments of the head and tail domains of β-adducin were incubated with KI-IOVs. After washing and centrifuging to remove unbound fragments, membrane-bound protein was assayed for GST activity to determine the extent of adducin construct binding to the KI-IOVs.[36] Both intact GST–β-adducin and its GST-linked tail domain were found to associate avidly with the membrane preparations (Figure 2A), whereas the head domain of β-adducin showed little tendency to bind KI-IOVs. Moreover, increasing concentrations of intact adducin were found

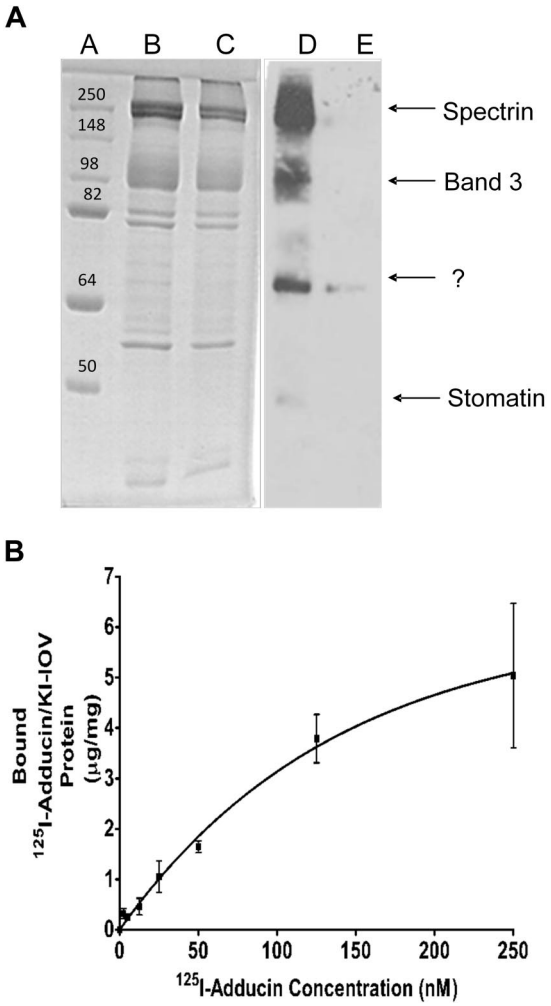

Figure 1. Adducin-binding proteins in KI-IOVs revealed by label transfer and copelleting experiments. (A) β-Adducin–binding proteins in IOVs revealed by label transfer experiments. Purified β-adducin tail (expressed in *E coli*) was incubated in the dark with a 2-fold molar excess of sulfo-SBED for 3 hours at 4°C, after which the protein solution was dialyzed overnight against PBS to remove unbound sulfo-SBED. IOVs (200 μg protein) were incubated with the above labeled β-adducin tail for 1 hour at room temperature in the dark to allow membrane association, after which cross-linking to nearest neighbor proteins was activated on ice by exposure for 15 minutes to a 302-nm light source (18.4 W) at a distance of 5 cm. A total of 10 mM dithiothreitol was then added to reduce the disulfide linkage between sulfo-SBED–adducin and its membrane anchor, and the labeled membrane anchor containing the transferred biotin was analyzed by SDS-PAGE, followed by transfer to nitrocellulose and visualization with streptavidin–horseradish peroxidase. Coomassie blue–stained gel lanes A through C contain molecular weight standards (lane A), or IOVs incubated with labeled β-adducin tail either in the absence (lane B) or presence (lane C) of a 20-fold excess of unlabeled β-adducin tail to competitively block all adducin binding sites on the IOVs. Lanes D and E represent streptavidin–horseradish peroxidase blots of lanes B and C. (B) KI-IOVs (100 μg) were incubated with increasing amounts of ^{125}I-adducin (purified from mature erythrocytes) or ^{125}I-BSA (60 μL total volume) for 2 hours at room temperature in a buffer consisting of phosphate-buffered saline containing 10% sucrose, protease inhibitor mixture, 1 mg/mL BSA, and no Mg^{2+}. Bound proteins were separated by centrifugation through a 25% sucrose cushion and quantified by γ counting. The BSA control was subtracted. Data points represent mean ± SD, n = 2. An apparent K_D of approximately 100 nM was calculated assuming a noncooperative, single site–binding equilibrium.

to quantitatively inhibit binding of β-adducin tail domain to KI-IOVs with a K_I approximately 150 nM (Figure 2B). Taken together, these data suggest that the tail domain of β-adducin constitutes a region of the adducin heterodimer that binds to the erythrocyte membrane.

To evaluate whether the domain specificity of β-adducin binding to KI-IOVs is similar to the domain specificity of β-adducin binding to band 3, the GST fusions of the 2 major β-adducin domains were also examined for their association with the purified His-tagged cdb3 in a standard nickel bead pull-down assay. Not surprisingly, immobilized cdb3 was found to pull down both intact β-adducin and β-adducin tail, but not β-adducin head domain (Figure 2A). Moreover, to ensure that the GST and His tags exerted no impact on the binding assay, the tags were reversed and GST-tagged cdb3 was used to pull down His-tagged β-adducin tail. As shown in Figure 2C, β-adducin tail was specifically copelleted with the cytoplamic domain of band 3, but not with either the cytoplasmic domain of glycophorin C or GST alone. Quantitation of the cdb3–adducin interaction by surface plasmon resonance revealed a binding affinity of approximately 80 nM, a value close to that obtained in the aforementioned KI-IOV binding assay.

To obtain further verification that band 3 indeed constitutes the primary binding site of β-adducin on the membrane, increasing concentrations of anti-cdb3 antibody were added to KI-IOVs in an effort to selectively obstruct β-adducin's access to band 3. As seen in Figure 2D, GST–β-adducin binding was strongly inhibited by the antibody to band 3, suggesting that few non–band 3 sites exist for β-adducin on KI-IOV's membranes.

In the course of the above binding studies, it was observed that β-adducin's affinity for band 3 was sensitive to the concentration of Mg^{2+}. Thus, as seen in Figure 2E, adducin's association with cdb3 is minimal in the absence of Mg^{2+}, but maximal at more than 3 mM Mg^{2+}. This sensitivity may be physiologically important, because it offers a possible mechanism for regulation of the band 3–adducin bridge in vivo. Thus, although total Mg^{2+} in erythrocytes is approximately 4 mM,[37] free Mg^{2+} can range from approximately 0 to 4 mM due to binding and release of Mg^{2+}-2,3-bisphosphoglycerate from deoxyhemoglobin during oxygenation cycles.[38] If such changes in free Mg^{2+} were to modulate the attachment of the junctional complex to the membrane in vivo (see below), they could exert an impact on membrane mechanical functions during oxygenation cycles. Indeed, we have observed that membrane preparations containing cation chelators (eg, EDTA [ethylenediaminetetraacetic acid]) have compromised adducin bridges, and prolonged incubation in such chelators can lead to release of adducin from the membrane (data not shown).

Because the sequence of β-adducin is similar to that of α-adducin (66%),[35,39] we next examined whether α-adducin might also bind band 3. Initial studies showed no interaction between the head domain of α-adducin and either KI-IOVs or cdb3 (data not shown). However, increasing concentrations of α-adducin tail were found to associate at least as avidly with immobilized cdb3 as β-adducin. Thus, as shown in Figure 3, immobilized cdb3 bound α-adducin tail in a saturable manner with a K_D approximately 35 nM plus or minus 7 nM, whereas neither immobilized ovalbumin nor inactivated and underivatized Affi-Gel 15 showed any tendency to bind α-adducin tail.

Finally, to estimate the stoichiometry of adducin binding to band 3 under optimal conditions, a binding isotherm of GST–β-adducin tail to KI-IOVs was determined in the presence of 4 mM Mg^{2+}. As shown in supplemental Figure 2, β-adducin tail was found to saturate KI-IOV binding sites at approximately 1.7 nmol adducin/mg KI-IOV protein. Assuming that band 3 constitutes approximately one-third of the total KI-IOV protein, the stoichiometry of adducin binding to band 3 at saturation can be estimated at approximately 0.5 adducins per band 3. Curiously, ankyrin binding to band 3 saturates at a stoichiometry of 0.25 ankyrins per band 3.[40]

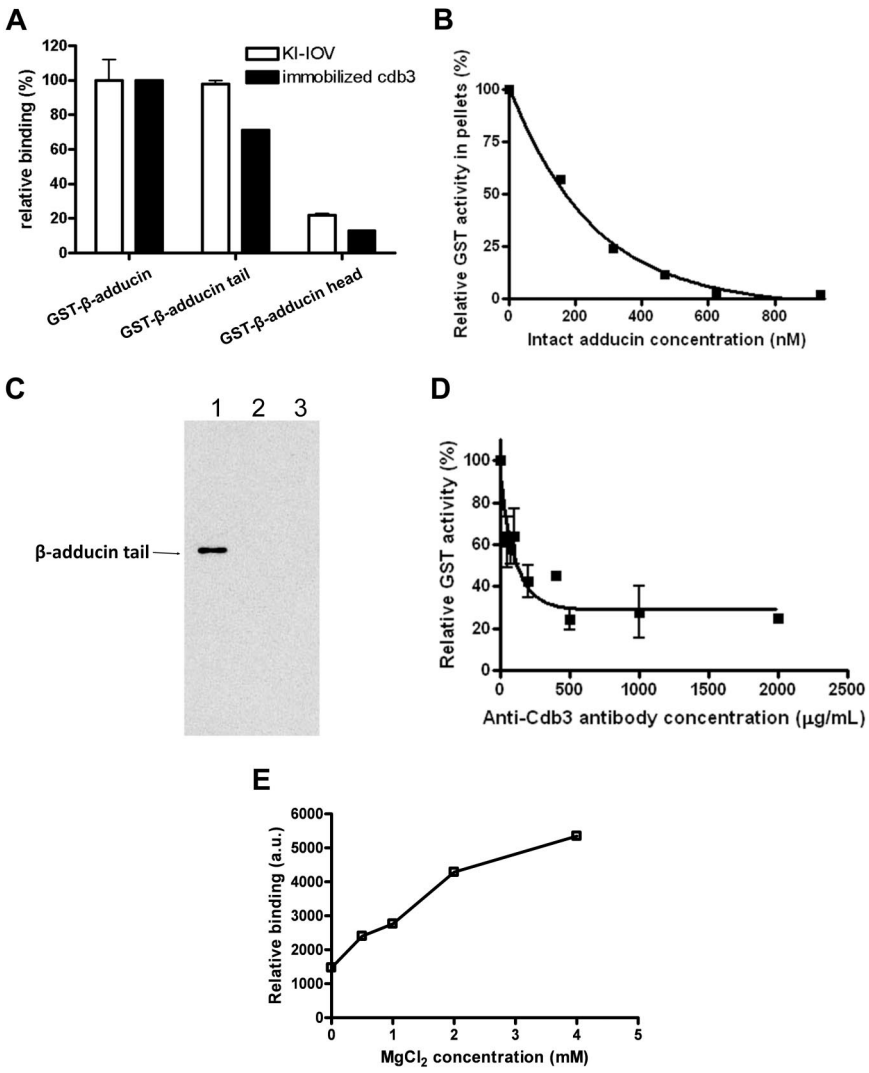

Figure 2. Identification of the adducin domain that interacts with KI-IOVs and band 3. (A) Native GST fusion constructs of intact adducin and its domains (1 μM) were incubated overnight at 4°C with KI-IOVs (65 μg in 200 μL; □) or with cdb3-$(His)_6$ (5.5 μM; ■). The KI-IOV suspension was pelleted through a 25% sucrose cushion, whereas the cdb3-$(His)_6$ solution was captured on nickel-nitrilotriacetic acid beads, washed 4 times, and eluted with 250 mM imidazole. GST activity was then quantified as a measure of adducin content. Data points represent mean ± SD, n = 2. Data were independently confirmed by dot blot analysis with anti-GST (data not shown). (B) Competitive inhibition of GST–β-adducin tail binding to KI-IOVs by intact erythrocyte adducin. KI-IOVs (100 μg of protein) were incubated with increasing amounts of intact erythrocyte adducin for 4 hours at 4°C (100 μL total volume), after which GST–β-adducin tail (250 nM) was added and incubated overnight at 4°C. Samples were processed and quantitated, as described above. Data points represent mean ± SD, n = 2 (apparent K_i ~150 nM). (C) Verification of β-adducin tail binding with cdb3 by GST pull-down assay. GST-tagged cytoplasmic domain of band 3 was coupled to glutathione beads, pelleted, and washed (as described above). His-tagged C terminus of β-adducin was added to the mixture. The GST–band 3–conjugated beads (lane 1) at a final concentration of 1 μM were incubated for 1 hour at room temperature, pelleted, and then washed. The pellet was analyzed by SDS-PAGE, and β-adducin fragment was detected by Western blotting using anti-His antibody. GST-tagged cytoplasmic domain of glycophorin C (lane 2) and GST alone (lane 3) were used as negative controls. (D) Competitive inhibition of GST–β-adducin tail binding to KI-IOVs by anti-cdb3 antibody. KI-IOVs (70 μg, 200 μL total volume) were incubated with increasing amounts of anti-cdb3 antibody for 4 hours at 4°C, after which GST–β-adducin tail (1500 nM) was added and incubated overnight at 4°C. Samples were processed and GST activity was quantitated, as described above. Data points represent mean ± SD, n = 2. (E) The association of GST–β-adducin tail with band 3 requires Mg^{2+}. His-tagged band 3 was immobilized on nickel beads and incubated with 270 nM GST–β-adducin tail in the presence of increasing concentrations of $MgCl_2$. Beads were pelleted, washed 5 times, and eluted with 250 mM imidazole in PBS. Eluted proteins were transferred to nitrocellulose membranes and probed for GST–β-adducin tail with an anti-GST polyclonal antibody. a.u. represents arbitrary units.

Adducin retention in band 3–deficient membranes

It has often been observed that a deficiency in one erythrocyte membrane protein will lead to reduced levels of its interacting partners. Therefore, we measured the amount of adducin in intact erythrocytes from band 3–null mice. As seen in Figure 4, genetic deletion of band 3 (see description of new band 3–null mouse in "Methods") leads to a concomitant reduction in erythrocyte α-adducin content of approximately 35%. This decrease in adducin suggests that either the polypeptide's trafficking to the membrane during erythropoiesis is compromised or its stability on the membrane is reduced by the absence of band 3. Importantly, adducin expression levels in other tissues harvested from the same band 3 knockout mice were found to be normal (data not shown).

Resealing of the α- and β-adducin tail domains into erythrocyte membranes reduces band 3 retention in derived membrane skeletons and lowers membrane stability

To evaluate the hypothesis that the adducin–band 3 bridge to the junctional complex is important to membrane structure, the impact of rupturing the band 3–adducin anchor on the stability of the membrane was examined. For this purpose, α- and β-adducin tail domains were resealed into leaky erythrocytes in the presence of 4 mM Mg^{2+} and allowed to competitively disrupt the endogenous band 3–adducin bridge. The modified resealed erythrocytes were then examined for changes in size and morphology by phase-contrast microscopy. As shown in Figure 5A, erythrocytes resealed with increasing concentrations of α-adducin tail underwent mild, but definite morphologic changes that were dose dependent, with nearly half of the cells showing some degree of altered morphology by 12 μM α-adducin tail. More importantly, when β-adducin tail domains (3-12 μM) were similarly resealed into leaky erythrocytes in the presence of 4 mM Mg^{2+}, almost all cells were observed to vesiculate within 1 hour (Figure 5B), suggesting that the band 3–adducin bridge contributes measurably to stabilizing cohesive forces connecting the bilayer and the membrane skeleton.

To confirm that the resealed adducin tail domains could indeed weaken the erythrocyte membrane by disrupting the band 3–adducin bridge, we next resealed α- and β-adducin tail domains into leaky erythrocyte ghosts and examined retention of band 3 in their detergent-extracted membrane skeletons. As shown in Figure 6A, detergent extraction of ghosts resealed with α-adducin tail yielded membrane skeletons containing 37% less band 3 than untreated controls. Interestingly, protein 4.1 and glycophorin C were also reduced in the detergent-extracted skeletons (~ 22% and 17%, respectively), suggesting they may also depend in part on α-adducin for association with the junctional complex. In contrast, other membrane proteins, especially those at the ankyrin complex

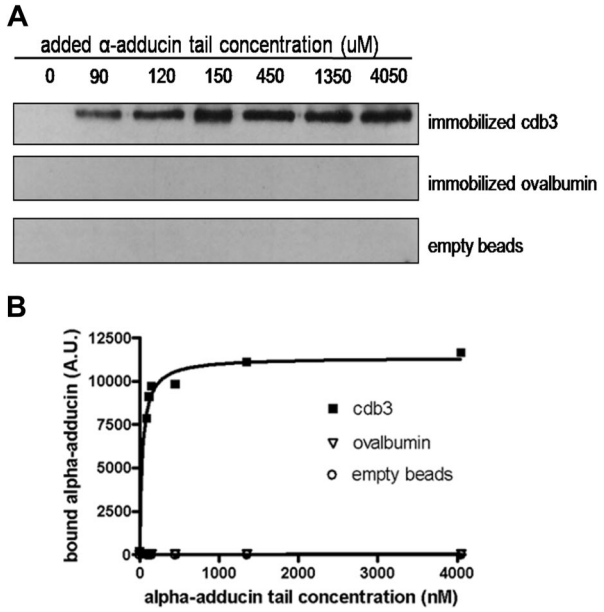

Figure 3. Concentration dependence of α-adducin tail binding to immobilized cdb3. Cytoplasmic domain of band 3, ovalbumin, or no protein was reacted with Affi-Gel 15 beads, as described in "Binding of α-adducin tail to cdb3 immobilized on Affi-Gel 15." Different concentrations of His-tagged α-adducin tail were incubated with the protein-derivatized beads for 4 hours at 4°C with gentle shaking. Beads were pelleted, washed 3 times with PBS, eluted, separated electrophoretically by SDS-PAGE, and analyzed by Western blotting using anti–α-adducin antibody (A). Quantitative densitometry was performed using Image J, and the resulting data were fit to a noncooperative single site-binding equilibrium, which yielded an apparent K_D of 35 ± 7 nM (B). A.U. indicates arbitrary units.

(eg, ankyrin, CD47, and glycophorin A), showed no reduction in skeletal retention, suggesting that the α-adducin tail fragment was selective in its displacement of proteins at the junctional complex.

Unfortunately, because resealing of β-adducin tail into leaky erythrocytes in the presence of 4 mM Mg^{2+} caused rapid vesiculation (Figure 5B), we were forced to study the effect of resealing β-adducin tail in the absence of Mg^{2+}. In these experiments, we found that band 3 retention in detergent-extracted skeletons was

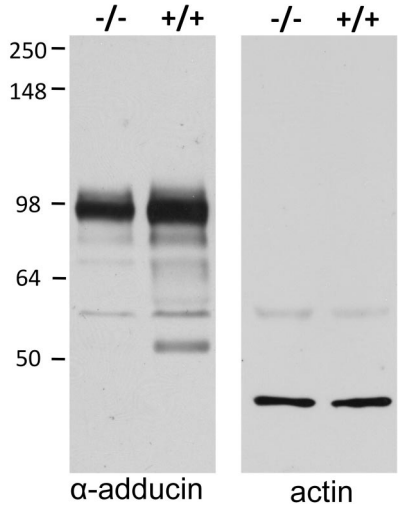

Figure 4. Intact band 3–null erythrocytes have reduced adducin content. Intact erythrocytes from wild-type (+/+) and band 3–null (−/−) mice were washed, plunged into 5× SDS-PAGE sample buffer, separated by SDS-PAGE, blotted onto nitrocellulose, and visualized with antibodies to adducin (left) and actin (right). Quantitative densitometry of 2 independent samples demonstrates a 35% decrease in adducin content of −/− erythrocytes.

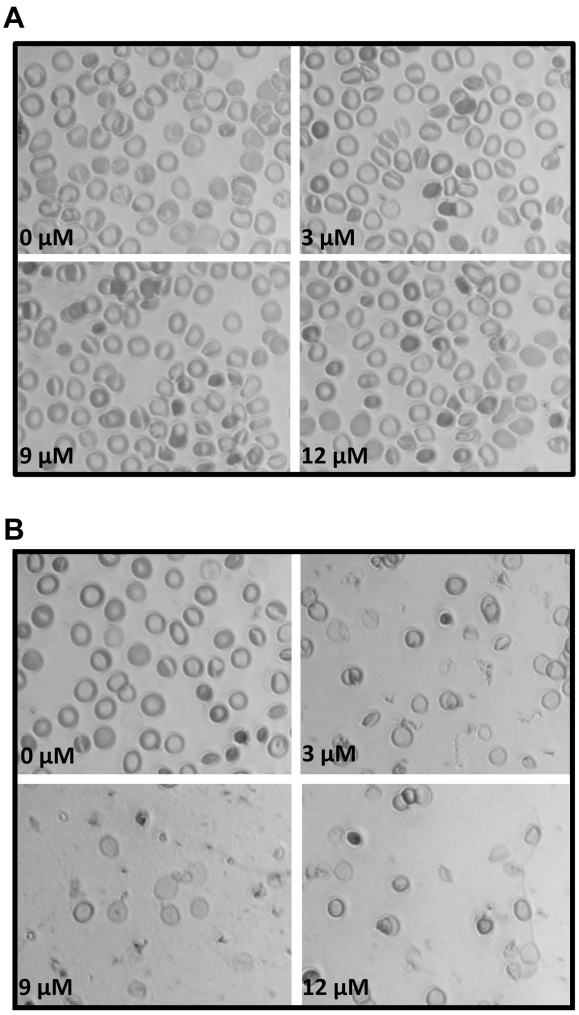

Figure 5. Analysis of the morphology of erythrocytes resealed in the presence of α- and β-adducin tail domains. Increasing concentrations of (A) α- and (B) β-adducin tail domains (0-12 μM) were incubated for 1 hour on ice with leaky erythrocytes (500 μL) at 50% Hct and then resealed for 45 minutes at 37°C in PBS containing 4 mM $MgCl_2$.

reduced by an average of 38% compared with untreated controls (Figure 6B). Whereas protein 4.1 and glycophorin C were also partially displaced by β-adducin tail, albeit to a lesser extent (~ 28% and 30%, respectively), these data still suggest a substantial fraction of the skeletally attached band 3 may be linked to the spectrin skeleton via adducin, and that fragments of both tail domains of adducin can disrupt this bridge. Because all skeletally anchored band 3 had been previously thought to be linked to ankyrin, this observation requires a revision of our current model of erythrocyte membrane structure.

Discussion

Identification of adducin as a critical bridge between the spectrin/actin junctional complex and the erythrocyte membrane bilayer raises important questions regarding adducin's possible role in regulation of membrane properties. Thus, the tail region of adducin that was shown to bind band 3 also caps actin filaments at the barbed end and binds Ca^{2+}/calmodulin.[28-30] Interaction of this tail domain with calmodulin reduces both actin binding and adducin-mediated enhancement of the spectrin–actin interaction.[29] Adducin

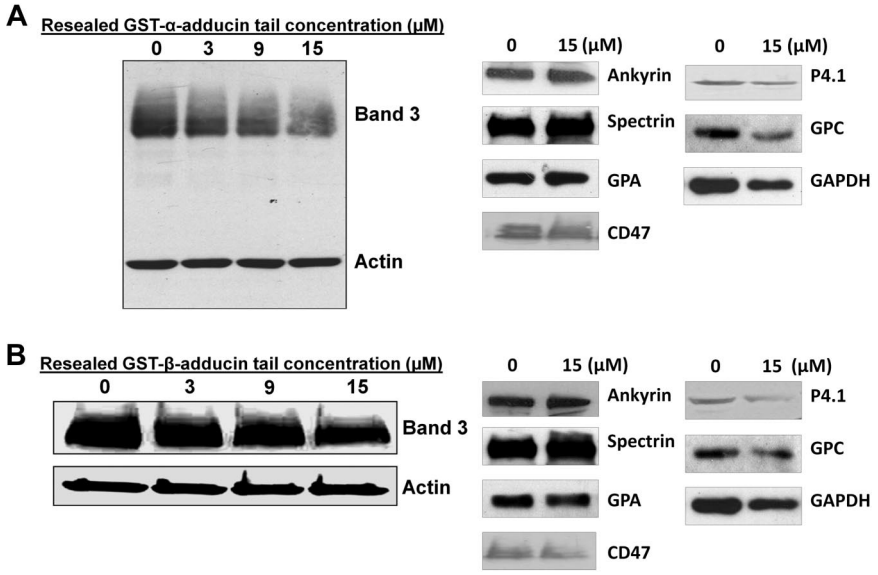

Figure 6. Effect of increasing concentrations of α- and β- adducin tail domains on retention of band 3 in detergent-extracted membrane skeletons. (A) Increasing concentrations of α-adducin tail were incubated for 1 hour on ice with leaky ghosts (5 mg/mL protein). Mg^{2+} was then added to a final concentration of 4 mM, and the leaky ghosts were incubated for another 30 minutes. Ghosts were resealed in PBS for 45 minutes at 37°C and then extracted in 1% Triton X-100 (final concentration). Pelleted skeletons were analyzed by SDS-PAGE and immunoblotting using anti–band 3 and anti-actin antibodies. Densitometry of band 3/actin ratios revealed a reduction in band 3 content of 0%, 25%, 33%, and 37% in extracted membrane skeletons from red cells resealed with 0 μM, 3 μM, 9 μM, and 15 μM α-adducin tail, respectively. Whereas no change in spectrin, ankyrin, CD47, or glycophorin A retention was observed, protein 4.1, glycophorin C, and GAPDH content in the skeletons were reduced approximately 22%, 17%, and 31%, respectively. (B) Increasing concentrations of GST–β-adducin tail were incubated for 4 hours on ice with leaky erythrocytes (3 mg/mL protein) and then resealed for 45 minutes at 37°C. Resealed cells were extracted in 2% Triton X-100 (final concentration), and skeletons were analyzed by SDS-PAGE, followed by immunoblotting with anti-cdb3 and anti-actin antibodies. Densitometry of band 3/actin ratios indicate ~ 50% ± 8% reduction in band 3 content at 15 μM GST–β-adducin tail, n = 2. Densitometry of band 3/actin ratios revealed a reduction in band 3 content of 0%, 17%, 21%, and 38% in extracted membrane skeletons from red cells resealed with 0 μM, 3 μM, 9 μM, and 15 μM β-adducin tail, respectively. Whereas no change in spectrin, ankyrin, CD47, or glycophorin A retention was observed, protein 4.1, glycophorin C, and GAPDH content in the skeletons was reduced ~ 28%, 30%, and 25%, respectively.

is also a substrate of protein kinase A, protein kinase C, and rho kinase,[41,42] and a basic stretch of amino acids within the COOH-terminal tail domains of both α- and β-adducin shows strong homology to myristoylated alanine-rich C-kinase substrate protein.[35] Whereas adducin's ability to cap actin filaments is reduced by protein kinase C phosphorylation, Rho kinase phosphorylation enhances its interaction with F-actin.[42] Considered together with the observation that band 3 binds adducin within this highly regulated region, one can posit that the band 3–adducin bridge might be subject to regulation by multiple signaling pathways.

Documentation that up to half of the skeletally attached band 3 population is associated with adducin and that this population provides a second bridge to the spectrin/actin cytoskeleton can explain many previously perplexing observations. First, prior identification of 3 populations of band 3 based on their distinct rotational mobilities[43] and sedimentation coefficients[44] can now be explained by an ankyrin-attached, adducin-attached, and freely diffusing band 3 population. Second, the observation that deletion of the ankyrin binding site on band 3 yields erythrocytes with only partially reduced stability can now be understood by recognizing that up to half of the band 3 bridges to the cytoskeleton remain intact in these mutated cells.[14] This same observation can also explain why the fraction of cytoskeletally attached band 3 is only reduced by approximately 60% in transgenic erythrocytes that express the defective band 3–ankyrin interaction.[40] Third, the recent puzzling observations that Rh proteins and protein 4.2, that is, established binding partners of band 3,[45] are both situated at least in part at the junctional complex are now consistent with localization of a fraction of band 3 at this same complex. Fourth, the aforementioned findings that membrane mechanical properties remain unperturbed after rupture of the glycophorin C–protein 4.1 bridge[8] and that reconstitution of the spectrin–actin binding domain of protein 4.1 into 4.1/glycophorin C–deficient membranes restores membrane mechanical properties without re-establishing the glycophorin C–protein 4.1 bridge[26,27] are clarified by recognizing that the band 3–adducin interaction, and perhaps a newly discovered dematin–glucose transporter 1 interaction,[46] provide important stabilizing bridges to the junctional complex.

Whereas the above enigmatic observations can now be explained by a band 3–adducin bridge to the membrane skeleton, data on the impact of complete deletion of adducin on erythrocyte membrane stability remain somewhat perplexing. Thus, erythrocytes from transgenic mice lacking all adducin subunits exhibit features characteristic of hereditary spherocytosis, with most cells displaying a "significant loss of surface area, decreased mean corpuscular volume, cell dehydration, and increased osmotic fragility."[47] This relatively mild phenotype can be contrasted with the phenotype of erythrocytes from ankyrin null mice, which fragment spontaneously in vivo, yielding a peripheral blood count dominated by circulating reticulocytes.[48] Why the band 3–ankyrin bridge appears more critical to membrane stability is unclear, but the possibility that other bridges to the junctional complex might also contribute to stabilization of this membrane-to-skeleton interaction should not be ignored. Moreover, it should be remembered that selective deletion of the ankyrin-binding loop on band 3 also generates a transgenic mouse with only a mild spherocytic anemia,[14] even though the band 3–ankyrin interaction is completely abrogated by this mutation (ie, perhaps suggesting that even the ankyrin-bridging complex might be stabilized by additional links to the membrane[49]). Finally, the simple stoichiometry of components argues that a more prominent role for the band 3–ankyrin interaction in membrane stability might be expected. Thus, most estimates place the number of ankyrin monomers and adducin dimers/cell at 100 000 and 30 000, respectively.[50] If each of these

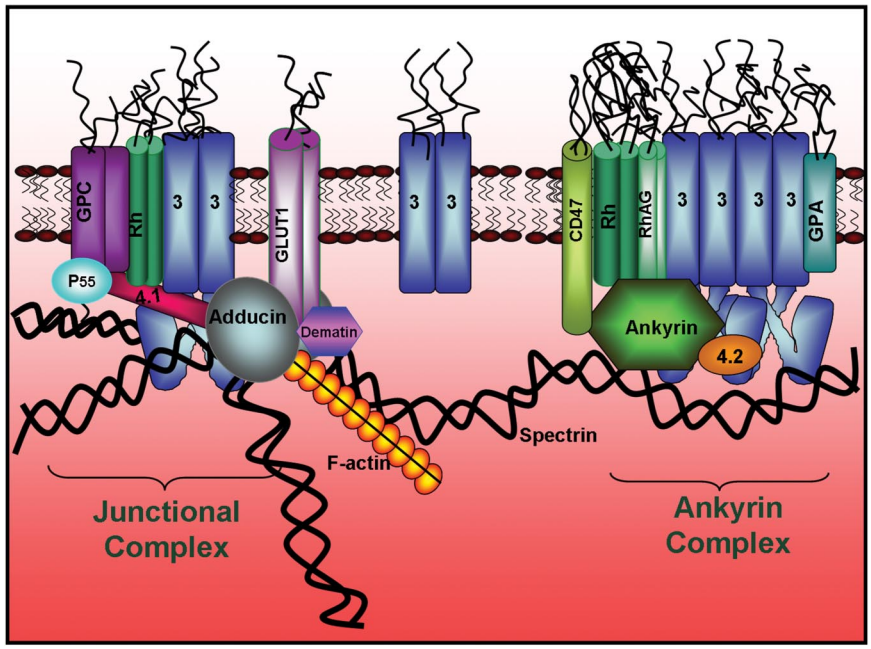

Figure 7. Revised model of the human erythrocyte membrane. Model shows the newly established band 3-to-adducin bridge to the junctional complex and the segregation of skeletally anchored band 3 into 2 distinct populations, one at the junctional complex and the second near the center of the spectrin tetramer where ankyrin binds.

bridging molecules were to bind one band 3 oligomer, there would have to be 3 times more band 3–ankyrin bridges than band 3–adducin bridges to stabilize the membrane.

Finally, because all current hematology and cell biology texts present inaccurate models of the red cell membrane, we offer a new model of the human erythrocyte membrane that incorporates our current understanding of erythrocyte membrane architecture (Figure 7). In this model, 2 major membrane protein complexes serve to anchor the spectrin/actin cytoskeleton to the phospholipid bilayer: (1) an ankyrin-bridged complex that contains membrane-spanning proteins band 3, glycophorin A, Rh complex proteins, and CD47, in addition to the peripheral proteins ankyrin, protein 4.2, and a variety of glycolytic enzymes,[45] and (2) a junctional complex that contains the membrane-spanning proteins band 3, glycophorin C, Rh complex proteins, and a glucose transporter, in addition to peripheral proteins actin, tropomyosin, tropomodulin, adducin, dematin, p55, protein 4.1, protein 4.2, and a variety of glycolytic enzymes.[45,46] Together, these 2 major protein complexes and their bridges to the spectrin/actin skeleton are most likely responsible for the prominent morphologic and mechanical properties of the cell.

Acknowledgments

We thank Vann Bennett for generously sharing his constructs of α- and β-adducin with us.

This work was supported by National Institutes of Health Grant GM24417-29.

Authorship

Contribution: P.S.L., W.A.A., T.F., and H.C. designed the experiments and analyzed the data; P.S.L., W.A.A., N.M., T.L.W., H.C., and T.F. all contributed to the writing of the manuscript; W.A.A., T.F., H.C., T.L.W., and X.A. performed experiments; E.E.D. and D.M.B. generated the band 3 null mouse, anemic mouse blood, and all mouse tissues; and all authors reviewed the manuscript.

Conflict-of-interest disclosure: The authors declare no competing financial interests.

Correspondence: Philip S. Low, Purdue University, Department of Chemistry, 560 Oval Dr, West Lafayette, IN 47907-2084; e-mail: plow@purdue.edu.

References

1. Alberts B, Johnson A, Lewis J, Roberts K, Walter P, Baff M. *Molecular Biology of the Cell.* 5th Ed. New York, NY: Garland Science Publishing; 2008.
2. Beutler E, Lichtman MA, Coller BS, Kipps TJ, Seligshon, U. *Williams Hematology*. 6th Ed. New York, NY: McGraw-Hill Professional; 2000.
3. Cooper GM, Hausman RE. *The Cell: A Molecular Approach.* 3rd Ed. Washington, DC: ASM Press; 2004.
4. Greer JP, Foerster J, Lukens JN, Rodgers GM, Paraskevas F, Glader B. *Wintrobe's Clinical Hematology.* 11th Ed. Baltimore, MD: Lippincott Williams & Wilkins; 2003.
5. Metzler DE. *Biochemistry: The Chemical Reactions of the Living Cells.* Vol 1. 2nd Ed. New York, NY: Academic Press; 2001.
6. Rodak BF, Fritsma GA, Doig K. *Hematology: Clinical Principles and Applications.* 2nd Ed. St. Louis, MO: Saunders; 2007.
7. Stamatoyannopoulos G, Majerus PW, Perlmutter RM, Varmus R. *The Molecular Basis of Blood Diseases.* 3rd Ed. Philadelphia, PA: Saunders; 2000.
8. Chang SH, Low PS. Regulation of the glycophorin C-protein 4.1 membrane-to-skeleton bridge and evaluation of its contribution to erythrocyte membrane stability. *J Biol Chem.* 2001;276: 22223-22230.
9. Lux SE. Dissecting the red cell membrane skeleton. *Nature.* 1979;281:426-429.
10. Bennett V. The molecular basis for membrane-cytoskeleton association in human erythrocytes. *J Cell Biochem.* 1982;18:49-65.
11. Bennett V, Healy J. Organizing the fluid membrane bilayer: diseases linked to spectrin and ankyrin. *Trends Mol Med.* 2008;14:28-36.
12. Costa FF, Agre P, Watkins PC, et al. Linkage of dominant hereditary spherocytosis to the gene for the erythrocyte membrane-skeleton protein ankyrin. *N Engl J Med.* 1990;323:1046-1050.
13. Lux SE, Tse WT, Menninger JC, et al. Hereditary spherocytosis associated with deletion of human erythrocyte ankyrin gene on chromosome 8. *Nature.* 1990;345:736-739.
14. Stefanovic M, Markham NO, Parry EM, et al. An 11-amino acid β-hairpin loop in the cytoplasmic domain of band 3 is responsible for ankyrin binding in mouse erythrocytes. *Proc Natl Acad Sci U S A.* 2007;104:13972-13977.
15. Van Dort HM, Knowles DW, Chasis JA, Lee G, Mohandas N, Low PS. Analysis of integral membrane protein contributions to the deformability and stability of the human erythrocyte membrane. *J Biol Chem.* 2001;276:46968-46974.

16. Chang SH, Low PS. Identification of a critical ankyrin-binding loop on the cytoplasmic domain of erythrocyte membrane band 3 by crystal structure analysis and site-directed mutagenesis. *J Biol Chem.* 2003;278:6879-6884.
17. Mohler PJ, Bennett V. Ankyrin-based cardiac arrhythmias: a new class of channelopathies due to loss of cellular targeting. *Curr Opin Cardiol.* 2005; 20:189-193.
18. Mohler PJ, Splawski I, Napolitano C, et al. A cardiac arrhythmia syndrome caused by loss of ankyrin-B function. *Proc Natl Acad Sci U S A.* 2004;101:9137-9142.
19. Mohler PJ, Rivolta I, Napolitano C, et al. Nav1.5 E1053K mutation causing Brugada syndrome blocks binding to ankyrin-G and expression of Nav1.5 on the surface of cardiomyocytes. *Proc Natl Acad Sci U S A.* 2004;101:17533-17538.
20. Scotland P, Zhou D, Benveniste H, Bennett V. Nervous system defects of AnkyrinB$^{-/-}$ mice suggest functional overlap between the cell adhesion molecule L1 and 440-kD AnkyrinB in premyelinated axons. *J Cell Biol.* 1998;143:1305-1315.
21. Marfatia SM, Lue RA, Branton D, Chishti AH. In vitro binding studies suggest a membrane-associated complex between erythroid p55, protein 4.1, and glycophorin C. *J Biol Chem.* 1994; 269:8631-8634.
22. Manno S, Takakuwa Y, Mohandas N. Modulation of erythrocyte membrane mechanical function by protein 4.1 phosphorylation. *J Biol Chem.* 2005; 280:7581-7587.
23. Mohandas N, Chasis JA. Red blood cell deformability, membrane material properties and shape: regulation by transmembrane, skeletal and cytosolic proteins and lipids. *Semin Hematol.* 1993; 30:171-192.
24. Reid ME, Takakuwa Y, Conboy J, Tchernia G, Mohandas N. Glycophorin C content of human erythrocyte membrane is regulated by protein 4.1. *Blood.* 1990;75:2229-2234.
25. Gascard P, Cohen CM. Absence of high-affinity band 4.1 binding sites from membranes of glycophorin C- and D-deficient (Leach phenotype) erythrocytes. *Blood.* 1994;83:1102-1108.
26. Discher D, Parra M, Conboy JG, Mohandas N. Mechanochemistry of the alternatively spliced spectrin-actin binding domain in membrane skeletal protein 4.1. *J Biol Chem.* 1993;268:7186-7195.
27. Takakuwa Y, Tchernia G, Rossi M, Benabadji M, Mohandas N. Restoration of normal membrane stability to unstable protein 4.1-deficient erythrocyte membranes by incorporation of purified protein 4.1. *J Clin Invest.* 1986;78:80-85.
28. Hughes CA, Bennett V. Adducin: a physical model with implications for function in assembly of spectrin-actin complexes. *J Biol Chem.* 1995; 270:18990-18996.
29. Mische SM, Mooseker MS, Morrow JS. Erythrocyte adducin: a calmodulin-regulated actin-bundling protein that stimulates spectrin-actin binding. *J Cell Biol.* 1987;105:2837-2845.
30. Kuhlman PA, Hughes CA, Bennett V, Fowler VM. A new function for adducin: calcium/calmodulin-regulated capping of the barbed ends of actin filaments. *J Biol Chem.* 1996;271:7986-7991.
31. Peters LL, Swearingen RA, Andersen SG, et al. Identification of quantitative trait loci that modify the severity of hereditary spherocytosis in wan, a new mouse model of band-3 deficiency. *Blood.* 2004;103:3233-3240.
32. Southgate CD, Chishti AH, Mitchell B, Yi SJ, Palek J. Targeted disruption of the murine erythroid band 3 gene results in spherocytosis and severe haemolytic anemia despite a normal membrane skeleton. *Nat Genet.* 1996;14:227-230.
33. Matsuoka Y, Li X, Bennett V. Adducin: structure, function and regulation. *Cell Mol Life Sci.* 2000; 57:884-895.
34. Sinard JH, Stewart GW, Stabach PR, Argent AC, Gilligan DM, Morrow JS. Utilization of an 86 bp exon generates a novel adducin isoform (β4) lacking the MARCKS homology domain. *Biochim Biophys Acta.* 1998;1396:57-66.
35. Joshi R, Gilligan DM, Otto E, McLaughlin T, Bennett V. Primary structure and domain organization of human α and β adducin. *J Cell Biol.* 1991;115:665-675.
36. Habig WH, Pabst MJ, Jakoby WB. Glutathione S-transferases: the first enzymatic step in mercapturic acid formation. *J Biol Chem.* 1974;249: 7130-7139.
37. Millart H, Durlach V, Durlach J. Red blood cell magnesium concentrations: analytical problems and significance. *Magnes Res.* 1995;8:65-76.
38. Weber RE, Voelter W, Fago A, Echner H, Campanella E, Low PS. Modulation of red cell glycolysis: interactions between vertebrate hemoglobins and cytoplasmic domains of band 3 red cell membrane proteins. *Am J Physiol.* 2004;287: R454-R464.
39. Joshi R, Bennett V. Mapping the domain structure of human erythrocyte adducin. *J Biol Chem.* 1990;265:13130-13136.
40. Yi SJ, Liu SC, Derick LH, et al. Red cell membranes of ankyrin-deficient nb/nb mice lack band 3 tetramers but contain normal membrane skeletons. *Biochemistry.* 1997;36:9596-9604.
41. Matsuoka Y, Hughes CA, Bennett V. Adducin regulation: definition of the calmodulin-binding domain and sites of phosphorylation by protein kinases A and C. *J Biol Chem.* 1996;271:25157-25166.
42. Kimura K, Fukata Y, Matsuoka Y, et al. Regulation of the association of adducin with actin filaments by Rho-associated kinase (Rho-kinase) and myosin phosphatase. *J Biol Chem.* 1998;273:5542-5548.
43. Che A, Morrison IEG, Pan R, Cherry RJ. Restriction by ankyrin of band 3 rotational mobility in human erythrocyte membranes and reconstituted lipid vesicles. *Biochemistry.* 1997;36:9588-9595.
44. Scheuring U, Kollewe K, Haase W, Schubert D. A new method for the reconstitution of the anion transport system of the human erythrocyte membrane. *J Membr Biol.* 1986;90:123-135.
45. Salomao M, An X, Zhang X, et al. Protein 4.1R-dependent multi-protein complex: new insights into the structural organization of the red blood cell membrane. *Proc Natl Acad Sci U S A.* 2008; 105:8026-8031.
46. Khan AA, Hanada T, Mohseni M, et al. Dematin and adducin provide a novel link between the spectrin cytoskeleton and human erythrocyte membrane by directly interacting with glucose transporter-1. *J Biol Chem.* 2008;283:14600-14609.
47. Robledo RF, Ciciotte SL, Gwynn B, et al. Targeted deletion of α-adducin results in absent β- and γ-adducin, compensated hemolytic anemia, and lethal hydrocephalus in mice. *Blood.* 2008; 112:4298-4307.
48. Rank G, Sutton R, Marshall V, et al. Novel roles for erythroid Ankyrin-1 revealed through an ENU-induced null mouse mutant. *Blood.* 2009;113: 3352-3362.
49. Bruce LJ, Ghosh S, King MJ, et al. Absence of CD47 in protein 4.2-deficient hereditary spherocytosis in man: an interaction between the Rh complex and the band 3 complex. *Blood.* 2002; 100:1878-1885.
50. Bennett V. The membrane skeleton of human erythrocytes and its implications for more complex cells. *Annu Rev Biochem.* 1985;54:273-304.